Sensors and Actuators A 147 (2008) 425–429

Contents lists available at ScienceDirect

Sensors and Actuators A: Physical

journal homepage: www.elsevier.com/locate/sna

Highly sensitive mass sensor using film bulk acoustic resonator

Re-Ching Lin [a], Ying-Chung Chen [a], Wei-Tsai Chang [a], Chien-Chuan Cheng [b], Kuo-Sheng Kao [c,*]

[a] Department of Electrical Engineering, National Sun Yat-Sen University, Kaohsiung, Taiwan
[b] Department of Electrical Engineering, De Lin Institute of Technology, Taipei, Taiwan
[c] Department of Computer and Communication, Shu-Te University, Kaohsiung, Taiwan

ARTICLE INFO

Article history:
Received 15 February 2008
Received in revised form 31 March 2008
Accepted 4 May 2008
Available online 16 May 2008

Keywords:
Mass sensor
ZnO
FBAR

ABSTRACT

Film bulk acoustic resonators (FBAR) have recently been adopted as alternatives to surface acoustic wave (SAW) in high frequency devices, due to their inherent advantages, such as low insertion loss, high power handling capability and small size. FBAR device can also be one of the standard components as mass sensor applications. FBAR sensors have high sensitivity, good linearity, low hysteresis and wide adaptability. In this study, a highly sensitive mass sensor using film bulk acoustic resonator was developed. The device structure of FBAR is simulated and designed by the Mason model, and fabricated using micro electromechanical systems (MEMS) processes. The fabricated FBAR sensor exhibits a resonant frequency of 2442.188 MHz, measured using an HP8720 network analyzer and a CASCADE probe station. Experimental results indicate that the mass loading effects agree with the simulated ones. Results of this study demonstrate that the sensitivity of the device can be achieved as high as 3654 Hz cm^2/ng.

1. Introduction

Film bulk acoustic resonators (FBAR) have recently been adopted as alternatives to surface acoustic wave (SAW) in high frequency applications, due to their inherent advantages, such as low insertion loss, high power handling capability and small size. FBAR device can also be one of the standard components as mass sensor applications, owing to its high sensitivity, good linearity, low hysteresis and wide adaptability [1–4]. The bulk acoustic wave (BAW) mass sensor of quartz crystal microbalance (QCM) typically operates at a frequency of less than 100 MHz because of the minimum thickness of quartz crystal. The relatively high resonant frequency of an FBAR device is the main reason for its higher mass sensitivity than that of a QCM sensor [5–7].

A high Q resonator, providing a precise frequency, is essential for highly sensitive sensor applications. The micro masses can be easily detected by the frequency variation of the mass sensors operating in the GHz range. The resonant frequency of FBAR above GHz, which is 100 times that of the QCM, makes it a candidate for nanotechnology application. Therefore, this study will investigate the varied frequency spectra of FBAR caused by additional deposited material on resonant zone.

An FBAR sensor has a sturdier structure than traditional sensors, and can be integrated with IC processes. Several piezoelectric materials, such as zinc oxide (ZnO), aluminum nitride (AlN) and lead zirconium titanate (PZT), have been applied to fabricate film bulk acoustic wave devices. Lead-related material is the best for the high electromechanical coefficient, but restricted to the issues of contamination. AlN has a high acoustic velocity, but a low electromechanical coefficient. On the other hand, ZnO piezoelectric thin film is widely adopted because of its high *c*-axis preferred orientation, high electrical resistivity (>10^6 Ω cm), moderate bulk acoustic velocity and electromechanical coefficient. Furthermore, the fabrication process of ZnO is compatible with standard Si fabrication technology, making it one of the most promising materials for fabricating film bulk acoustics resonators (FBARs) [8–10].

In this study, the structure of an FBAR mass sensor was simulated and constructed to investigate the mass loading effects. The characteristics of the electrodes and ZnO piezoelectric layer are optimized for FBAR fabrication to enhance the mass sensor sensitivity. Finally, the sensitivity of the FBAR sensor for titanium mass loading is carried out.

2. Theory

Fig. 1(a) shows the schematic of an FBAR. It illustrates the composite structure of the top electrode, piezoelectric layer, bottom electrode and membrane. Fig. 1(b) shows the Mason equivalent cir-

* Corresponding author.
E-mail address: kks@mail.stu.edu.tw (K.-S. Kao).

0924-4247/$ – see front matter © 2008 Elsevier B.V. All rights reserved.
doi:10.1016/j.sna.2008.05.011

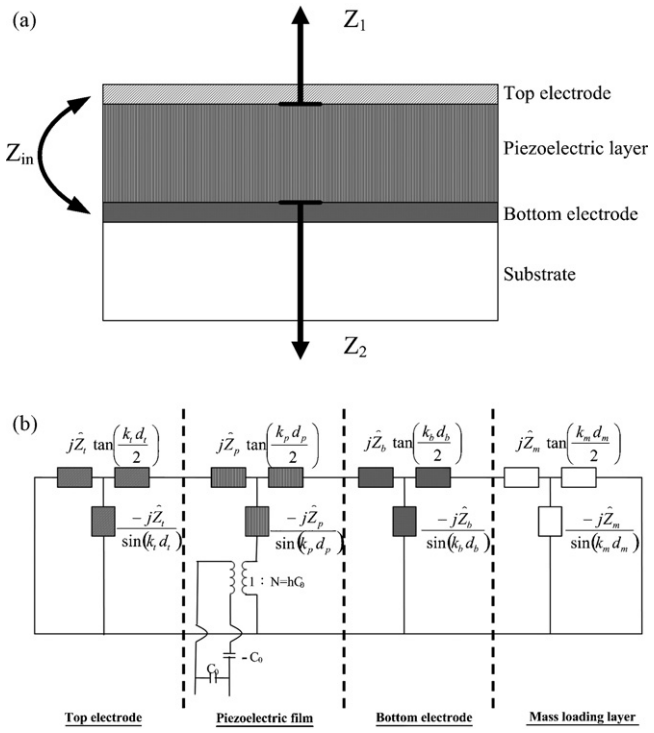

Fig. 1. (a) The schematic diagram of an FBAR resonator; (b) Mason equivalent circuit of an FBAR device.

cuit of an FBAR, where the equivalent impedance between top and bottom electrode is:

$$Z_{in} = \frac{1}{j\omega C_0}\left[1 - \frac{k_t^2}{\gamma_p}\frac{(z_1+z_2)\sin\gamma_p + j2(1-\cos\gamma_p)}{(z_1+z_2)\cos\gamma_p + j(1+z_1z_2)\sin\gamma_p}\right], \quad (1)$$

The impedance of Z_1 and Z_2 are given by

$$Z_1 = jZ_{e1}\tan\gamma_{e1} \quad (2)$$

$$Z_2 = j\frac{Z_m\tan\gamma_m + Z_{e2}\tan\gamma_{e2}}{1-(Z_m/Z_{e2})\tan\gamma_{e2}\tan\gamma_m}, \quad (3)$$

in which, Z_{e1}, Z_{e2} and Z_m denote the acoustic impedances of top electrode, bottom electrode and mass loading layer, respectively. The terms $z_1 = Z_1/Z_o$ and $z_2 = Z_1/Z_o$ are the equivalent impedances observed from the top surface and bottom surface of piezoelectric layer normalized to the acoustic impedance of piezoelectric layer Z_o, respectively. γ_{e1}, γ_{e2} and γ_m are the phase delay of the top electrode, bottom electrode and mass loading layer, respectively, and γ_p is phase delay of piezoelectric layer. The γ_{e1}, γ_{e2}, γ_m and γ_p are described as,

$$\gamma_{e1} = \frac{2\pi f l_{e1}}{v_{e1}} \quad (4)$$

$$\gamma_{e2} = \frac{2\pi f l_{e2}}{v_{e2}} \quad (5)$$

$$\gamma_m = \frac{2\pi f l_m}{v_m} \quad (6)$$

$$\gamma_p = \frac{2\pi f l_p}{v_p} \quad (7)$$

C_0 is the static capacitance between the top and bottom electrodes; l_p and v_p indicate the thickness and acoustic wave velocity of piezoelectric layer, respectively, and k_t^2 is the electromechanical coupling coefficient of piezoelectric layer, described as

$$k_t^2 = \left(\frac{\pi^2}{4}\right)\left(\frac{f_s}{f_p}\right)\left(\frac{f_p - f_s}{f_p}\right) \quad (8)$$

In Eq. (1), the impedance becomes infinite when

$$(z_1+z_2)\cos\gamma_p + j(1+z_1z_2)\sin\gamma_p = 0, \quad (9)$$

and

$$f = \left\{2\left(\frac{l_p}{v_p} + \frac{\rho_m l_m}{\rho_p v_p}\right)\right\}^{-1}, \quad (10)$$

where f is resonant frequency of resonator.

The resonant frequency of various modes can be evaluated from the materials parameters used in the FBAR. Table 1 lists the simulation parameters. To calculate and estimate the sensitivity of an FBAR device, the mass loading with regard to frequency is defined as follows:

$$\frac{\delta f}{f} \approx -\frac{\rho_d \delta l_d}{\rho_p l_p} = -\frac{\delta m}{m} \quad (11)$$

In this study, the sensitivity of an FBAR mass sensor is estimated based on Sauerbrey equation [11]:

$$S_m = \lim_{\delta m \to 0}\left(\frac{\delta f}{f}\right)\left(\frac{1}{\delta m}\right) \quad (12)$$

Table 1
Material parameters for FBAR sensor

	ρ (10^3 kg/m^3)	C_{33} (10^9 N/m^2)	v (10^3 m/s)	ε_{33}	k_t^2 (%)
ZnO	5.67	204.30	6.20	8.8	8.5
SiN_x	2.33	186.50	8.94	N.A.	N.A.
Pt	21.09	N.A.	2.68	N.A.	N.A.
Mo	10.28	N.A.	6.30	N.A.	N.A.
Al	2.70	N.A.	5.1	N.A.	N.A.

N.A.: not applicable.

3. Experimental

Silicon (1 0 0) wafers coated with low-stress silicon nitride layers (SiN_x/Si) were utilized as substrates, because low-stress silicon nitride can be adopted as supporting membranes in integrated FBAR devices. The SiN_x layer was stipulated to be grown by low-pressure chemical vapor deposition (LPCVD) to ensure low stress. The substrate was cleaned by the Radio Corporation of America (RCA) processes. The bottom electrode of Pt was deposited by DC magnetron sputtering to keep in step with the seed layer of Ti without substrate heating [12].

The piezoelectric thin film was deposited by reactive rf magnetron sputtering with two-step processes. The base pressure of sputtering system was evacuated to 2×10^{-6} Torr using diffusion pump. The working pressure and rf power were 15 mTorr and 80 W, respectively. The gas flow rate ratio (O_2/Ar + O_2) for the first and second steps were 75% and 50%, respectively [13].

Stress is inherent in the multi-layer structure. The piezoelectric layer in the fabrication process was deposited with heated substrate holder, making stress difficult to be avoided. However, the excess stress occurring at the cavity edge caused the etching stop layer of silicon nitride to fail. The etching process with KOH etching solution attacked from the stress unbalance region, causing the structure on the other side to collapse.

The two-step etching process was adopted to maximize the device yield. The high-speed wet-etching process was followed by dry-etching at a moderate speed. The dry-etching of reaction ion etching (RIE) is relatively mild for the cavity manufacture. The 2nd

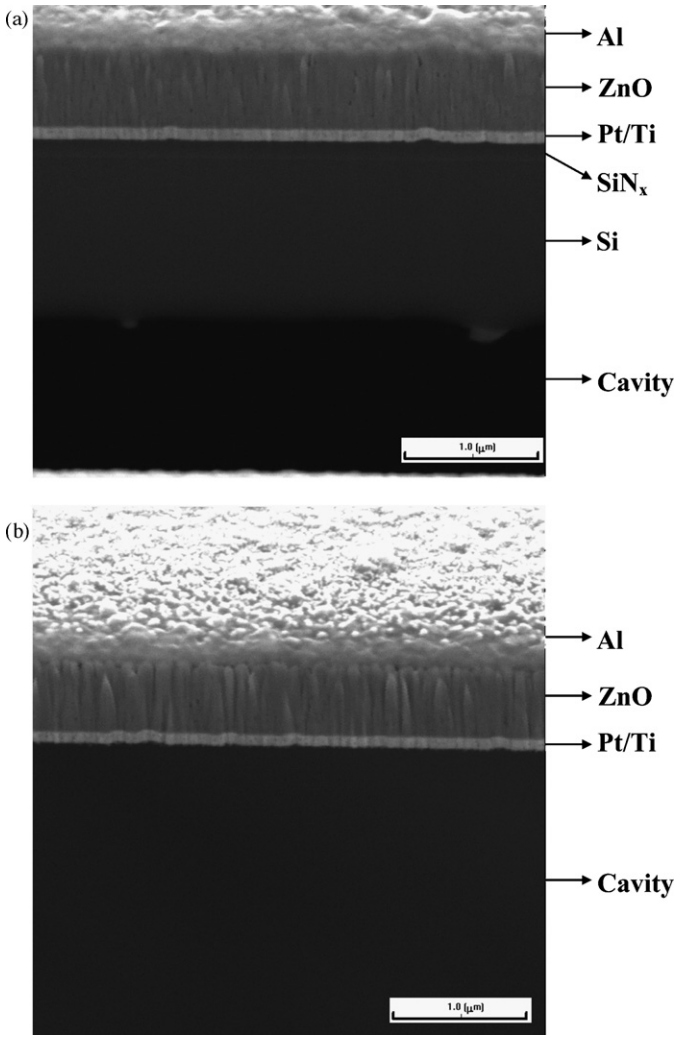

Fig. 2. SEM cross-sectional morphologies of an FBAR mass sensor etched by Focused Ion Beam (FIB), (a) with residual Si; (b) with residual Si etched by RIE.

step of RIE can reduce destructiveness caused by only performing KOH wet-etching [14]. Consequently, the cavity of FBAR is accomplished by a two-step process of wet-etching and dry-etching. Fig. 2 shows the SEM cross-sectional images of the FBAR mass sensor.

The preferred orientation and crystal properties of the ZnO film were measured by X-ray diffraction (XRD) using a SHIMADZU XRD-6000 with Cu Kα radiation. The cross-sections of the grain structure of ZnO films were observed by scanning electron microscopy (SEM) (Philips XL40 FESEM). The frequency responses of the FBAR devices were measured using the HP8720 network analyzer and CASCADE probe station (RHM-06/V + GSG 150).

4. Results and discussion

The bottom electrode of Pt/Ti with low surface roughness (0.69 nm), high conductivity (2.60 Ω/□), and good adhesion to substrate was first obtained. The top electrode of Al was deposited by DC sputter. The ZnO film with (0 0 2) preferred orientation and smooth surface roughness of 7.37 nm was also obtained by the two-step deposition process. Table 2 lists the fabrication parameters of each layer of the FBAR mass sensor. Figs. 3 and 4 show the *c*-axis orientation of ZnO thin film and surface image of ZnO/Pt/Ti/SiN_x/Si structure, which reveals the strong ZnO (0 0 2) preferred orientation and uniform surface. The results obtained indicate that ZnO

Table 2
Sputtering parameters of ZnO and metals

Parameters	ZnO		Metal		
	1st step	2nd step	Ti	Pt	Al
rf Power (W)	80	80	–	–	–
DC power (W)	–	–	250	200	75
$O_2/Ar + O_2$	75%	50%	–	–	–
Ar (sccm)	–	–	10	10	10
Pressure (mTorr)	15	15	20	5	3
Temperature (°C)	R. T.	R. T.	R. T.	R. T.	R. T.

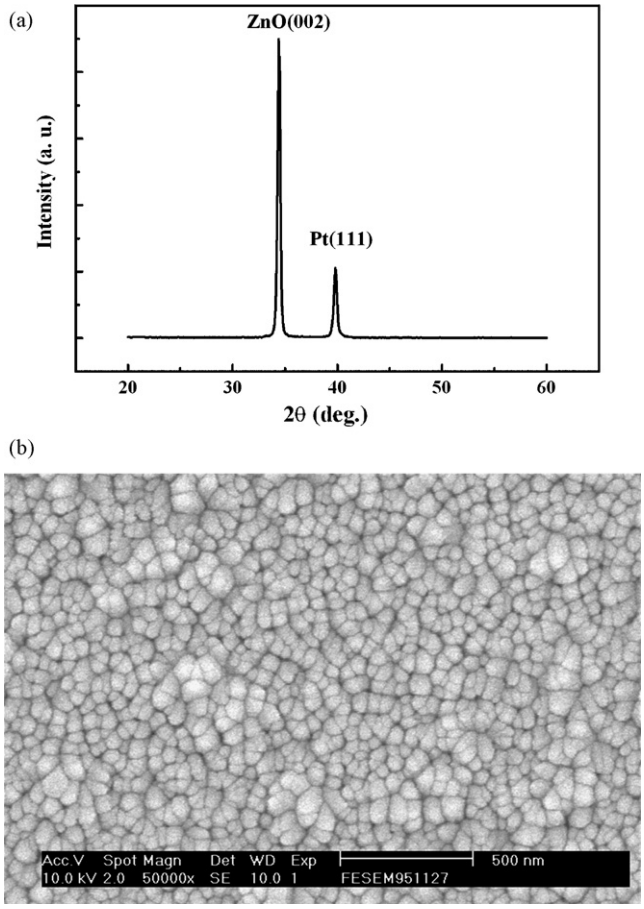

Fig. 3. (a) XRD pattern of ZnO film deposited on Pt/Ti/SiN_x/Si; (b) SEM image of ZnO film deposited on Pt/Ti/SiN_x/Si.

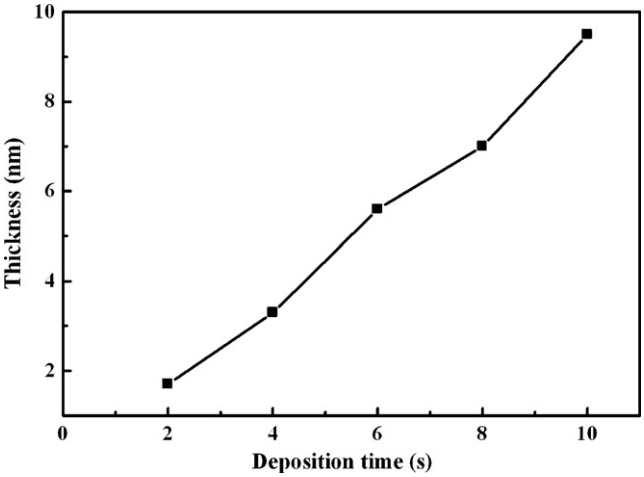

Fig. 4. Deposition rate of Ti metal measured by SEM.

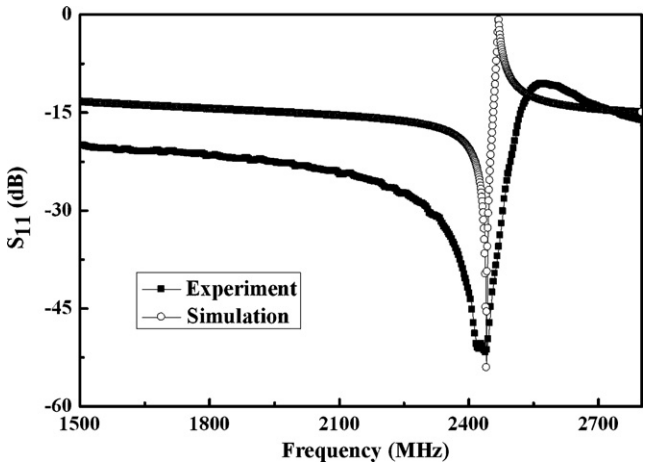

Fig. 5. Frequency responses of FBAR sensor with experiment and simulation.

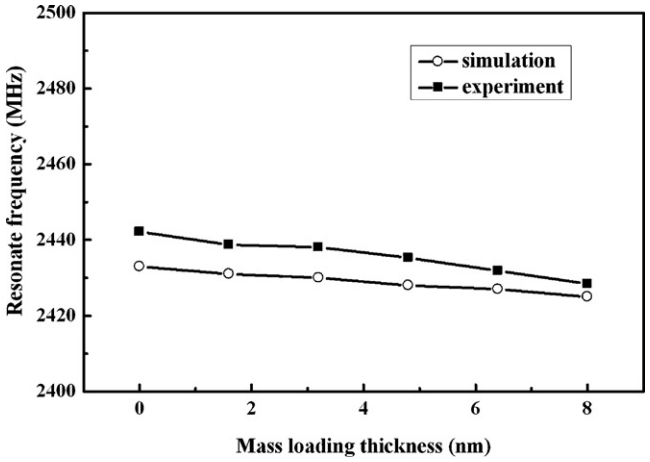

Fig. 7. Frequency variations under different mass loading.

film deposited with the two-step method exists a smooth and uniform surface, which will result in a high quality factor for FBAR [8].

Fig. 5 shows the simulated and experimental frequency responses of an FBAR device without mass loading. The resonant area of FBAR is 150 μm × 160 μm. Table 1 lists the material parameters adopted for device simulation. The frequency response of the FBAR device shows a center frequency of 2442.188 MHz and a return loss of −51.7 dB, respectively. Besides, the experimental results are consistent with those of simulated.

The mass loading layer of titanium (Ti) deposited by DC sputtering was adhered to the back cavity of FBAR device. The deposition rate shown in Fig. 4 was calculated to be 0.975 nm/s. The thickness of the mass loading layer was checked through the α-step and FESEM investigations. Fig. 6 shows the results of frequency response with mass loading. The center frequency decreased significantly as the thickness of mass loading increased from 1.6 to 8 nm. The thickness variations of loading layer caused the change in phase delay of the mass loading layer. As derived from Eq. (6), $\gamma_{ms} = 2\pi f l_{ms}/v_{ms}$ varied with the mass loading thickness l_{ms}. Therefore, the increased thickness of loading layer caused the resonant frequency of FBAR to shift. Additionally, the return loss of FBAR devices decreased with the increased mass loadings. This result can also be obtained from Eq. (3), where the impedance Z_2 increased with the increased γ_{ms}. Hence, the resonant frequency and return loss of FBAR decreased as the mass loading layer thickness increased.

Fig. 7 indicates that the resonant frequency decreased due to the mass loading effect as an excess layer was added to the cavity of FBAR device. High resonant frequency and compact structure with high film quality will cause the large frequency variation of FBAR mass sensor. In order to calculate the sensitivity, the excess film had been expressed by mass with nano gram, as showed in Fig. 8. The resonant frequency decreased with increased mass loading. The sensitivity, S_m, calculated from Eq. (12) is about 3654 Hz cm^2/ng. With the same mass loading, the frequency change in this study is 20 times larger than that of Zhang and Kim [15]. The mass sensitivity is extremely large as a result of the originality of FBAR structure in this study.

A typical FBAR structure includes top electrode, piezoelectric layer, bottom electrode and membranes. A membrane is a supporting layer to strengthen FBAR device structure. In this study, the two-step etching processes have been adopted to improve device yield. Although the membranes had been etched by RIE, the strong bottom electrode of Pt substituted as SiNx membranes. The originality of structure of FBAR mass sensor is shown in Fig. 2(b). Pt bottom electrode is not only a perfect bottom electrode but also a strong membrane layer. The optimized growth parameters of Pt bottom electrode had been disclosed in our previous report [12]. The increasing sensitivity depends on reducing the number of layer of FBAR mass sensor [16]. In this study, the membranes had been

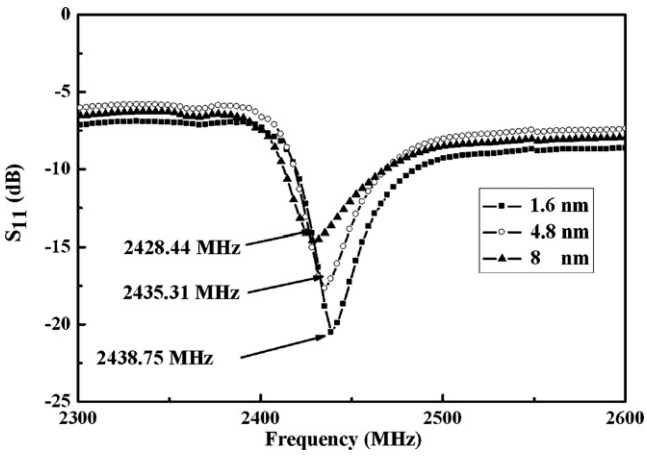

Fig. 6. Frequency responses of FBAR sensor with different mass loading.

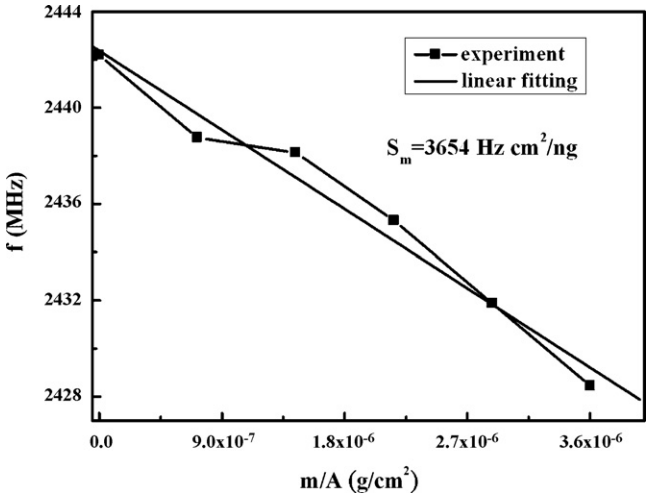

Fig. 8. Resonant frequency variations with various mass loading.

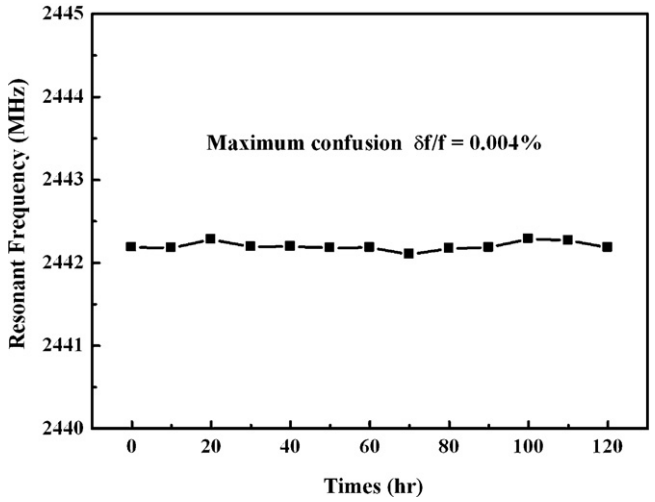

Fig. 9. The resonant frequency variation with measuring time.

removed leading to high mass sensitivity. The two-step etching process is not only improve the device yield but also increase the mass sensitivity.

The frequency stability is a key point of FBAR mass sensor. The noise in frequency measurement of FBAR mass sensor has been achieved in this study. The frequency variation with measuring time was shown in Fig. 9. The maximum variation rate ($\delta f/f_0$) of 0.004% of resonant frequency is calculated from Fig. 9. The influence of sensitivity degree of accuracy on FBAR mass sensor is negligible. Therefore, the stability of FBAR mass sensor has been expected in this study.

5. Conclusion

This work presents a highly sensitive mass sensor using ZnO-based FBAR. The influences on the FBAR characteristics due to the mass loading layer is investigated through simulation and experiment. The strength and electrical conductivity of the electrodes and the crystallization of the piezoelectric layer are all fundamental for FBAR mass sensor. The results indicate that FBAR has a wide frequency variation with a tiny mass loading. The Pt bottom electrode was successfully adopted to substitute for membranes. The highly sensitive FBAR mass sensor will have particular application to substitute for quartz and SAW sensors. Briefly, the two-step etching process and perfect bottom electrode provided high device yield as well as extremely high sensitivity.

Acknowledgment

The authors would like to thank the National Science Council of the Republic of China, Taiwan for financially supporting this research under contract No. NSC 96-2221-E-110-057, NSC 96-2221-E-237-002 and NSC 96-2221-E-366-006.

References

[1] K.M. Lakin, J. Belsick, J.F. McDonald, K.T. McCarron, Improved bulk wave resonator coupling coefficient for widebandwidth filters, IEEE Ultrason. Symp. Proc. 1 (2001) 827–831.
[2] K.W. Kim, G.Y. Kim, J.G. Yook, H.K. Park, Air-gap type TFBAR-based filter topologies, Microwave Opt. Technol. Lett. 34 (2002) 386–387.
[3] M. Aberg, M. Ylimaula, M. Ylilammi, T. Pensala, A. Rantala, A low noise 0.9 GHz FBAR clock, Analog Integr. Circuits Signal Process. 50 (2007) 29–37.
[4] B. Drafts, Acoustic wave technology sensors, IEEE Trans. Microwave Theory Tech. 49 (2001) 795–802.
[5] V.M. Mecea, Vibrating piezoelectric sensors, Sens. Actuators A 40 (1994) 630–637.
[6] R.P. O'Toole, S.G. Bums, G.J. Bastiaans, M.D. Porter, Thin aluminum nitride film resonators: miniaturized high sensitivity mass sensors, Anal. Chem. 64 (1992) 1289–1294.
[7] R. Gabl, E. Green, M. Schreiter, H.D. Feucht, H. Zeininger, R. Primig, D. Pitzer, G. Eckstein, W. Wersing, Novel integrated FBAR sensors: a universal technology platform for bio- and gas-detection, IEEE Sens. 2 (2003) 1184–1188.
[8] J.B. Lee, J.P. Jung, M.H. Lee, J.S. Park, Effects of bottom electrodes on the orientation of AlN films and the frequency responses of resonators in AlN-based FBARs, Thin Solid Films 447 (2004) 610–614.
[9] K.M. Lakin, Thin film resonators and filters, IEEE Ultrason. Symp. Proc. 2 (1999) 895–906.
[10] L. Mang, E. Hickernell, R. Pennell, T. Hickernell, Thin-film resonator ladder filter, IEEE Trans. Micro. Symp. 2 (1995) 887–890.
[11] G. Sauerbrey, Verwendung von Schwingquarzen zur Wägung dünner Schichten und zur Mikrowägung, Z. Phys. 155 (1959) 206–222.
[12] R.C. Lin, K.S. Kao, C.C. Cheng, Y.C. Chen, Deposition and structural properties of R.F. magnetron sputtered ZnO thin films on Pt/Ti/SiNx/Si substrate for FBAR device, Thin Solid Films 516 (2008) 5262–5265.
[13] R.C. Lin, K.S. Kao, Y.C. Chen, Two-step sputtered ZnO piezoelectric films for film bulk acoustic resonators, Appl. Phys. A 89 (2007) 475–479.
[14] R.C. Lin, P.T. Hsieh, Y.C. Chen, K.S. Kao, C.M. Wang, Effects of substrate residue on the frequency response of high-tone bulk acoustic resonator, IEEE Freq. Cont. Symp. (2007) 695–698.
[15] H. Zhang, E.S. Kim, Micromachined acoustic resonant mass sensor, IEEE Microelectromech. Syst. 14 (2005) 699–706.
[16] H. Zhang, W. Pang, E.S. Kim, High-frequency bulk acoustic resonant microbalances in liquid, IEEE Freq. Cont. Symp. (2005) 73–77.

Biographies

Re-Ching Lin was born in Yunlin County, Taiwan, ROC, on December 05, 1978. He received the MS degrees in Department of Physics from Tung Hai University, Taichung, Taiwan in 2003. Currently, he is a PhD student of electrical engineering from National Sun Yat-Sen University, Kaohsiung, Taiwan. His current research interests are in the field of piezoelectric material and film bulk acoustic wave devices.

Ying-Chung Chen was born in Tainan, Taiwan, ROC, on November 4, 1956. He received the MS and PhD degrees in electrical engineering from National Cheng Kung University, Tainan, Taiwan, in 1981 and 1985, respectively. Since 1983, he has been at National Sun Yat-Sen University, Kaohsiung, Taiwan. He is a professor of electrical engineering at National Sun Yat-Sen University. His current research interests are in the areas of electronic devices, surface acoustic wave devices, thin-film technology, and electronic ceramics. He is a member of the Chinese Society for Materials Science and a registered electrical engineer at Taiwan.

Wei-Tsai Chang was born in Kaohsiung city, Taiwan, ROC, on October 13, 1982. He received the MS degrees in Department of Physics from National Sun Yat-Sen University, Kaohsiung, Taiwan in 2007. Currently, he is a PhD student of electrical engineering from National Sun Yat-Sen University, Kaohsiung, Taiwan. His current research interests are in the field of piezoelectric material and film bulk acoustic wave devices.

Chien-Chuan Cheng was born in Keelung, Taiwan, ROC, on March 26, 1964. He received the MS and PhD degrees in electrical engineering from National Sun Yat-Sen University, Kaohsiung, Taiwan, in 1988 and 1995, respectively. Since 1990, he has been at De Lin Institute of Technology, Taipei, Taiwan. Currently, he is a professor of electronic engineering at De Lin Institute of Technology. His current research interests are in the areas of surface acoustic wave devices, electronic ceramics, and thin film technology.

Kuo-Sheng Kao was born in Chia-Yi City, Taiwan, ROC, on September 11, 1973. He received the MS and PhD degrees in electrical engineering from National Sun Yat-Sen University, Kaohsiung, Taiwan, in 1999 and 2004, respectively. Currently, he is an assistant professor of computer and communication at SHU-TE University, Kaohsiung, Taiwan. His current research interests are in the field of thin-film-based acoustic wave devices.